Available online at www.sciencedirect.com

ScienceDirect

Procedia Structural Integrity 78 (2026) 694–701

Structural Integrity
Procedia

www.elsevier.com/locate/procedia

XX ANIDIS Conference

# Experimental and numerical study on masonry barrel vault strengthened through CRM system: preliminary results

Marielisa Di Leto[a,] *, Filippo Campisi[a], Giuseppe Rusticano[a]
Calogero Cucchiara[a], Lidia La Mendola[a], Diego Antonio Trapani[a]

[a]*Department of Engineering, University of Palermo, Viale delle Scienze, Palermo, 90128, Italy*

**Abstract**

Masonry vaults are widespread in the ancient built environment; they frequently provide a load-bearing purpose and can have numerous variables that influence structural behaviour, e.g., shape, materials, and boundary conditions. These structures may require strengthening interventions to increase load-bearing capacity and minimise vulnerability. In the presence of masonry substrate, intervention approaches based on inorganic matrix composite materials are preferred. Despite their growing popularity, there are just a few experimental campaigns in the literature that employ these composite materials to reinforce curved surfaces.

The current study intends to contribute to this field by investigating the behaviour of barrel vaults composed of calcarenite stone masonry reinforced with Composite Reinforced Mortar (CRM). Specifically, the preliminary outcomes of the proposed experimental program will be presented. Simultaneously, a Finite Element (FE) model was calibrated in order to interpret the data and gain a better understand the phenomenology. The results obtained can provide useful hints for the design of this strengthening intervention.


Peer-review under responsibility of XX ANIDIS Conference organizers

*Keywords:* Masonry vaults; Strengthening; CRM; Experimental tests; Numerical results

* Corresponding author.
*E-mail address:* marielisa.dileto@unipa.it


Peer-review under responsibility of XX ANIDIS Conference organizers
10.1016/j.prostr.2025.12.089

## 1. Introduction

Masonry vaults, and in particular barrel vaults, are a distinctive element of historical architecture, especially widespread in the Mediterranean region. These curved structural systems are commonly found in monumental buildings, residential constructions, and masonry bridges. Their geometry allows for the spanning of large spaces and the efficient transfer of vertical loads, exploiting the excellent compressive strength of masonry, which compensates for its negligible tensile resistance. The behaviour of masonry vaults is, however, influenced by numerous factors, including their geometric configuration, construction techniques, mass distribution, boundary conditions, material degradation, and any alterations accumulated over time. Vaults may serve as load-bearing elements—supporting backfill or adjacent spandrels that transfer loads from upper floors—or as non-structural components, such as ceilings that carry only their self-weight (Boem & Gattesco (2021)). When subjected to gravity loads alone, the structural stability of these systems is generally ensured, provided that the line of thrust remains confined within the thickness of the vault.

In seismic contexts, their structural response becomes significantly more complex. Horizontal earthquake-induced forces may activate kinematic mechanisms that lead to progressive collapse, typically characterized by the formation of hinges along specific lines, depending on the boundary and support conditions. Such vulnerabilities have been widely documented in the literature (Ramaglia (2016), Cardinali (2023)) and continue to prompt renewed interest in the assessment and preservation of these structures, particularly through experimental testing of reinforcement techniques (Boem & Gattesco (2021), La Mendola et al. (2009), Marini et al. (2017), Gattesco et al. (2018), Caceres-Vilca et al. (2024)).

In response to the seismic vulnerability of vaulted structures, there is growing emphasis on the development of strengthening interventions that are both effective and compatible with historical masonry. Among the most studied retrofitting strategies are those based on fibre-reinforced composite materials, including Fibre-Reinforced Polymer (FRP), Textile-Reinforced Mortar (TRM), Fibre-Reinforced Cementitious Matrix (FRCM), and Composite Reinforced Mortar (CRM) systems (Alecci et al. (2016), Zampieri et al. (2018)). These systems have been shown to significantly improve structural capacity, both in terms of maximum load and ultimate displacement, and to enhance ductility, particularly in the case of inorganic matrix composites (Garmendia et al. (2015), De Santis et al. (2017), Carozzi et al. (2018), Boem & Gattesco (2023)).

While CRM systems have been thoroughly investigated in recent years for their application in reinforcing masonry panels under in-plane and out-of-plane actions, their use for the reinforcement of curved surfaces, such as barrel vaults, has only recently gained research attention (Boem & Gattesco (2021), Gattesco et al. (2018)). This shift reflects an urgent need for targeted solutions that can effectively prevent or mitigate hinge formation and reduce the probability of seismic-induced collapse in historic vaulted structures.

This paper presents the planned experimental campaign to study the effectiveness of reinforcement with CRM system when applied on the vault. The load test will be conducted by applying a vertical load to a quarter of the vault span. The experimental part was preceded by a prediction study, which was useful for the design of the entire experimental campaign and test set-up. The kinematic theorem of the limit analysis was used to estimate the residual load reached at the end of the test. At the same time a finite element model was developed using Midas FEA NX software (2022), with the aim of estimating the stiffness and maximum load reached during the experimental test on the unreinforced vault and the consequent modifications in the presence of reinforcement realised with the CRM system. The experimental results shown are preliminary results of a larger experimental campaign involving one test on an unreinforced vault and two tests on CRM-reinforced vault samples. The results on the experimental test carried out on the unreinforced vault sample were analysed and compared with the respective numerical results.

## 2. Experimental program

The experimental test described in this paper is part of a broader experimental program aimed at evaluating the effectiveness of CRM (Composite Reinforced Mortar) strengthening systems, both from seismic and thermal perspectives, when applied to masonry vaults. The program involves the construction of three masonry vaults: one unreinforced (to serve as a reference) and two reinforced trough CRM system. The material selected for the construction of the masonry vault specimens is calcarenite, a stone commonly used in historical buildings throughout the Mediterranean region. The specimens were designed to represent, at medium scale, typical features of existing historical structures. Each specimen consists of a barrel vault constructed using calcarenite blocks measuring 250 × 120 × 50 mm³, assembled with lime mortar. The masonry units were arranged with their longer sides oriented transversely, resulting in a vault thickness of 120 mm. The mortar joints were 10 mm thick. The vault had a span of 1920 mm, an intrados radius of 1000 mm, and a transverse width of 1030 mm (Fig. 1a). The vault specimen was constructed over two reinforced concrete support bases.

## 3. Materials and setup

The vault was constructed using calcarenite bricks and a lime–cement-based mortar. The specimen was designed to be representative of masonry barrel vaults commonly found in historical buildings throughout the Mediterranean region. It is important to note that the calcarenite employed in this study was sourced from the Sabucina quarry, located in Sicily. This lithotype is characterized by promising mechanical properties, described in detail below, which distinguish it from calcarenites extracted from other Sicilian quarries. Prior to testing, a comprehensive material characterization was performed. This included compression tests on eight cubic calcarenite stone specimens (70 mm sides), conducted in accordance with UNI EN standards (2006). The resulting average compressive strength was $f_c$ = 9.29 MPa. Calcarenite was also subjected to thermal testing using a method based on UNI EN 12664:2002 and UNI EN 12667:2002, yielding a thermal transmittance value of 1.763 W/m$^2$K. The M5-grade pre-mixed lime–cement mortar was tested after 28 days of curing, following UNI EN 1015:2006 Standards. Flexural strength tests were conducted on three prismatic mortar specimens (40 × 40 × 160 mm), which were then tested in compression. The mortar exhibited a compressive strength of $f_c$ = 5.28 MPa and a flexural strength of $f_f$ = 1.87 MPa. Additionally, three masonry wall specimens (510 × 530 × 120 mm) were tested in compression to determine the mechanical properties of the masonry assembly. The tests, conducted in accordance with ASTM standards (1997) provided an average compressive strength of $f_{c,M}$ = 7.62 MPa and a Young's modulus of E = 5576 MPa. The full-scale vault specimen was tested at the Structures and Materials Laboratory of the Engineering Department, University of Palermo (Italy). Figure 1b shows the setup of the testing apparatus.

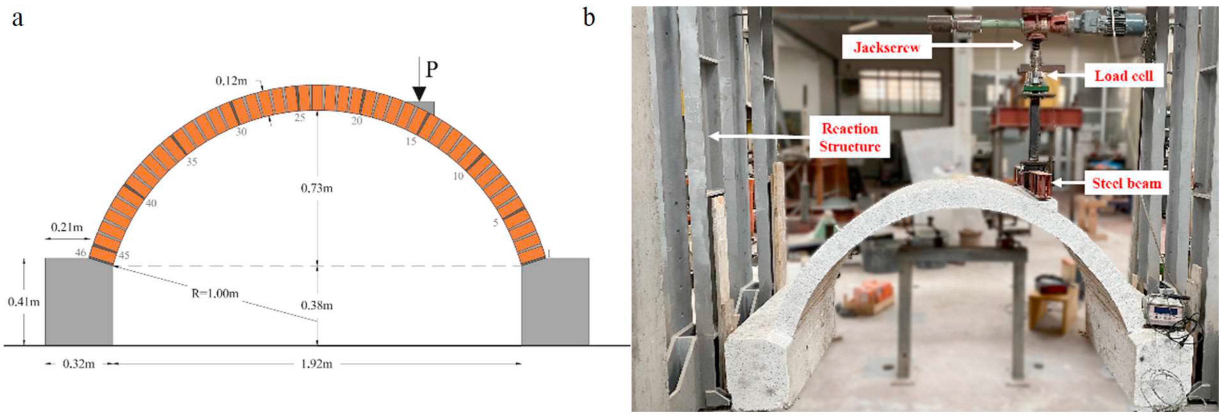


Fig. 1. Vault specimen: (a) Geometric details; (b) view of the specimen in the testing apparatus (front side).

The vault was installed within a steel reaction frame anchored to the laboratory's strong floor, which provided resistance to the reaction forces. The concrete base supports were positioned in contact with the column bases of the frame to prevent horizontal displacement. Loading was applied at a quarter-span location using a jackscrew operated at a constant displacement rate of 0.04 mm/s. A load cell placed between the jack and a transverse steel beam, used to ensure uniform load distribution, measured the applied force. The instrumentation setup was designed to capture both force and displacement data. Four digital displacement transducers were installed at the vault's intrados to monitor global vertical and horizontal displacements: one vertical and one horizontal were installed at the intrados at the load application point, while a similar pair was positioned at the intrados at the symmetrical point of the vault.

An additional eight displacement transducers were placed on the rear surface to track the opening of expected flexural hinges. The front face of the specimen was prepared for Digital Image Correlation (DIC) by applying a white background with a black speckle pattern. This enabled full-field monitoring of deformations across the entire surface of the vault and supporting piers, allowing the evolution of damage to be correlated with the applied loads.

## 4. Analytical and numerical previsions

Before the testing, Analytical and numerical prediction models were employed to estimate the maximum load reached during the test and to design the entire experimental setup.

### *4.1. Analytical prediction of ultimate load*

An analytical approach was adopted to estimate the collapse load of the masonry vault, based on the kinematic theorem of limit analysis (Heyman, 1966). The objective was to obtain a preliminary estimate of the load level at which failure was expected to occur, considering a vertical force applied at one-quarter of the span. To this end, several potential failure mechanisms were hypothesized by varying the locations of the absolute and relative centre of rotation along the intrados and extrados of the vault, denoted as $C_1$, $C_{12}$, $C_2$, $C_{23}$, and $C_3$. Each configuration represents a distinct collapse mechanism. Assuming a No-Tension Material (NTM), the principle of virtual work was applied to compute the corresponding collapse load. By comparing the results, the mechanism yielding the lowest collapse load was identified as the most critical, in accordance with the upper bound theorem. The configuration and hinge positions associated with this minimum value are shown in Fig. 2. The selected mechanism corresponds to a predicted collapse load of 2.32 kN.

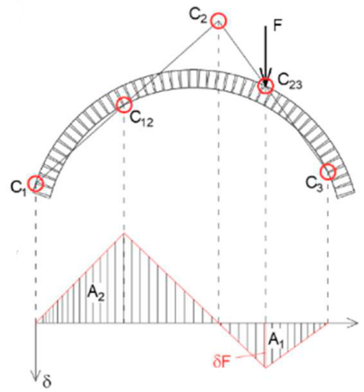


Fig. 2: Collapse mechanism under vertical load applied at one-quarter of the vault span: hinge positions and virtual vertical displacement diagram.

### *4.2. Finite Element Modelling*

A simplified micro-modelling strategy was adopted to simulate the structural behaviour of the masonry vault in both unreinforced and CRM-strengthened configurations (see Figure 3 (a) and (b)). Masonry units were modelled as continuous deformable elements, while the mortar joints were not explicitly represented. Instead, the interaction between adjacent blocks was captured through 6-node interface elements, simulating potential planes of cracking and sliding, in line with the discrete approach proposed by Lourenço (2010). Based on the geometric regularity of the barrel vault, defined by a circular directrix and parallel generatrixes, the three-dimensional problem was reduced to a two-dimensional model. The mesh consisted of 8-node quadrilateral shell elements with linear elastic behaviour and a Young’s modulus of 13249 MPa (Minafò & La Mendola, 2018), while nonlinearities were fully concentrated at the interfaces via a Discrete Cracking (DC) law.

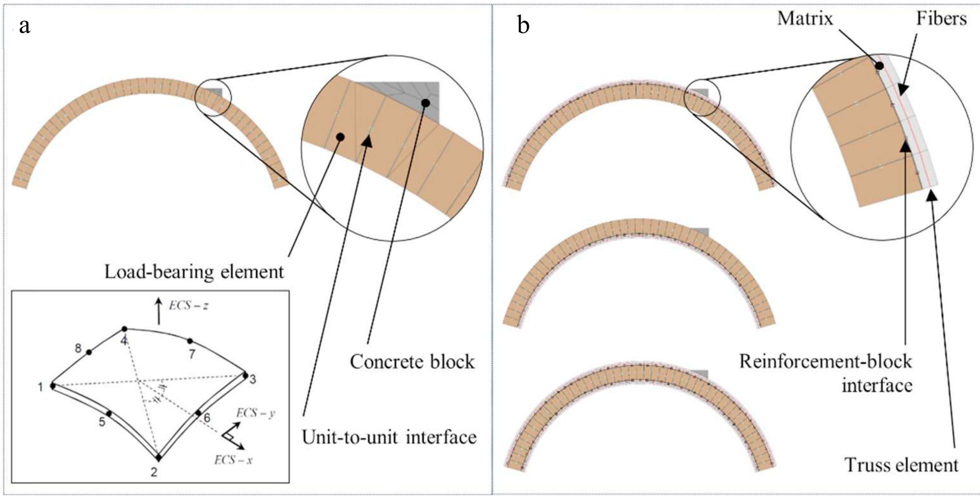


Fig. 3. 2D Finite Element models: (a) unreinforced vault; (b) reinforced vault in three different configurations: intrados, extrados, both intrados and extrados

In the numerical model the CRM system was positioned on the extrados and intrados, both separately and together, to quantify the numerical gains in load capacity and overall performance. Following the modelling strategy by Castellano et al. (2023), the composite reinforcement was idealized as a layered continuous system: the inorganic matrix was modelled using shell elements, and the G-FRP mesh was represented by 2-node truss elements resisting only axial tension. The mechanical properties relating to the definition of the non-linear behaviour of the reinforcement were assumed as they could not be obtained directly from experimental tests. The mechanical properties of the model's non-linear parameters, calibrated in accordance with the scientific literature, (Castellano et al. (2023), Lourenço, P. B., & Rots, J., (1994), Lourenço, P. B. (2010)), are as follows. (i) Unit-to-unit interface properties: normal stiffness modulus ($K_n$) equal to 57.38 N/mm$^3$, tangential stiffness modulus ($K_t$) equal to 22.95 N/mm$^3$, tensile strength ($f_t$) equal to 0.04 MPa and mode I fracture energy ($G_f^I$) equal to 0.0037 N/mm. (ii) Unit reinforcement interface properties: normal stiffness modulus ($K_n$) equal to 588.51 N/mm$^3$, tangential stiffness modulus ($K_t$) equal to 235.40 N/mm$^3$, tensile strength ($f_t$) equal to 0.05 MPa and mode I fracture energy ($G_f^I$) equal to 0.0046 N/mm.

The analyses provided numerical load–vertical displacement curves, as shown in Figure 4, for different configurations: Unreinforced Vault (UV), Reinforced Vault Intrados only (RV-I), Reinforced Vault Extrados only (RV-E) and Reinforced Vault Intrados and Extrados (RV-IE). The numerical results are consistent with values

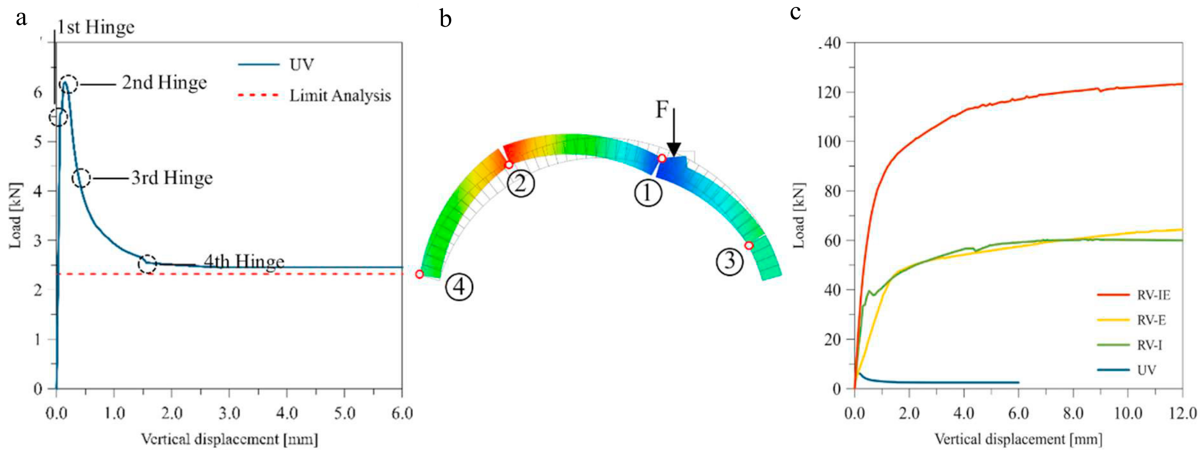


Fig. 4. (a) Load-displacement curve of the UV; (b) Failure mechanism of the UV at the ultimate load step and (c) load-displacements curves for the different reinforcement configurations.

reported in the literature, thereby supporting the validity of the adopted modelling approach. The unreinforced vault exhibits a four-hinge failure mechanism alternating between intrados and extrados, with the peak load reached at the formation of the second hinge. The numerical load–displacement curve reaches the analytically estimated collapse load, thus confirming the validity of the prediction, represented by the red dashed line at the value of 2.32 kN corresponding to the load evaluated though the limit state analysis.

In the numerical simulations, the interface properties were the primary variable, modified consistently with the mechanical characteristics of the mortar. The CRM system presence changes the failure mode and affects the structural response in terms of capacity curve. In all configurations, the linear elastic phase ends with the initiation of a crack beneath the load application point. When reinforcement is placed on the extrados, a sudden stiffness reduction occurs due to cracking at the intrados because of hinges opening. Conversely, intrados reinforcement delays crack formation, due to hinges opening, and stiffness degradation, proving more effective in the initial phase.

Compared to the brittle behaviour of the unreinforced case, the reinforced vault demonstrates a more ductile response. Reinforcement applied to both faces of the vault leads to the highest load-bearing capacity, as it prevents hinge formation at both the intrados and extrados, as expected. The simulations were carried out in order to evaluate the behaviour according to different configurations: in real applications in most cases, the choice of type is constrained by several factors, such as whether or not both surfaces can be worked on.

## 5. Experimental results and comparisons

Figure 5a shows the load–displacement curve for the unreinforced vault, which remained elastic up to load 4.51 kN and 0.08 mm displacement. Stiffness then decreased, with hinge formation illustrated in Figure 5b. A first hinge (Fig.5b-I) formed at the extrados with joints opening at intrados under the load point (5.00 kN), followed by a second (Fig.5b-II) at the intrados (5.42 kN) with joints opening at extrados. The test continued until a four-hinge collapse mechanism developed at 6.12 kN, involving the 1st (Fig.5b-IV), 17th (Fig.5b-I), 30th (Fig.5b-II), and 46th (Fig.5b-III) joints.

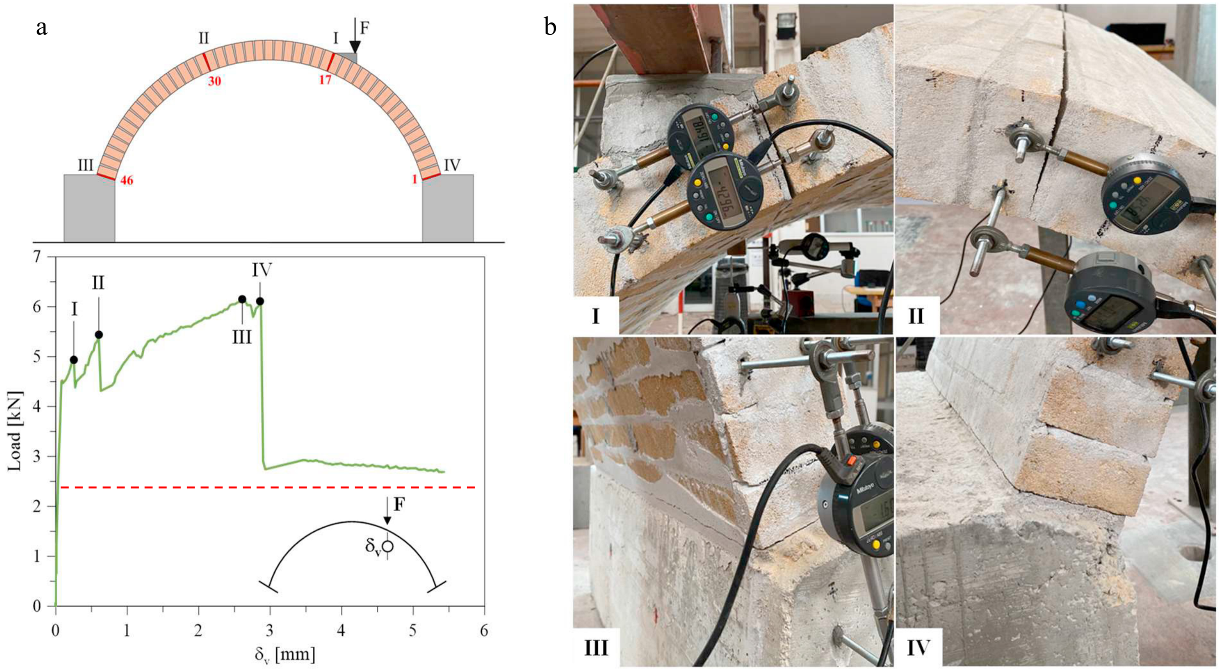


Fig. 5. (a) Load-displacement curve of the UV; (b) Four hinges developed.

After the collapse mechanism formed, the test continued to evaluate the residual capacity, stabilizing at 2.80 kN, close to the 2.32 kN previously predicted. Despite masonry's brittle nature, the load reached 6.12 kN at 2.61 mm displacement. In Figure 6b some of DIC analysis results are shown: curves representing displacements δ, are indicated by an acronym in which the second letter indicates the direction of the displacement (*v* for vertical and *h* for horizontal) and the third indicates the position of the pedicle on which it was recorded (*L* stands for left and *R* stands for right). The last curve in green *δv - Under load*, on the other hand, shows the measurements of the displacements under load, in order to relate the readings to the overall test curve.

The DIC analysis (see Figure 6b) revealed rotation of the left abutment, with upward and leftward shifts, while the right remained fixed. This asymmetry influenced the collapse mechanism, highlighting the effectiveness of DIC in capturing localized kinematics.

A direct comparison between the experimental measurements and the numerical predictions (Figure6a) from the micro-model of the unreinforced vault provides the following results: the experimental maximum load was 6.12 kN versus 6.21 kN of the numerical curve (1.5 % difference), the displacement at peak load reached 2.61 mm compared to 0.15 mm in the model (94 % difference, because of the rotation of abutments), the ultimate load was 2.80 kN against 2.45 kN predicted (13 % difference), and the experimentally determined stiffness of 56.43 kN/mm was 64 % lower than the numerical stiffness of 92.57 kN/mm.

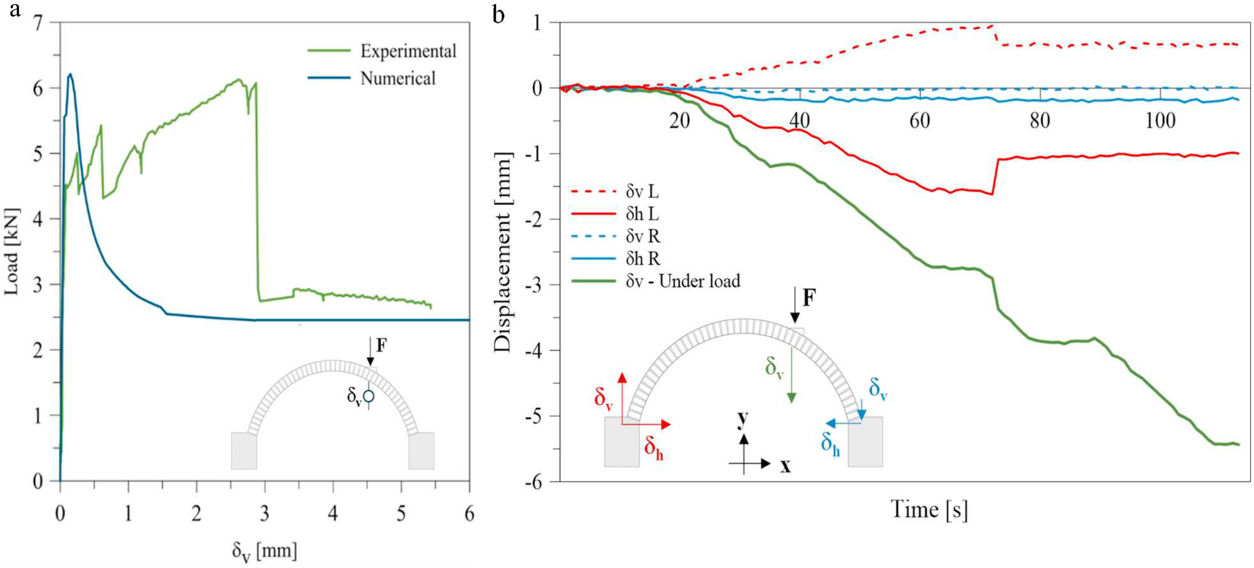


Fig.6. (a) Comparison between experimental and numerical load-displacement curves; (b) Load–time and displacement-time curves from DIC analysis.

## 6. Conclusions

This study numerically investigated the behaviour of a masonry vault in both unreinforced and reinforced configurations. The predictive results were compared with preliminary experimental data. Digital Image Correlation (DIC) proved to be effective for this type of application, where it is necessary to capture a continuous displacement field rather than discrete point measurements. DIC allowed for accurate correlation between load steps and hinge formation, as well as the identification and quantification of pier displacements, which in turn led to vault behaviour different from what was initially expected. Both analytical and numerical models were essential for designing the experimental setup. Specifically, the models successfully predicted the experimental collapse load, with the numerical simulation also providing a good approximation of the maximum load reached during the test. The numerical model of the reinforced configuration, although not yet validated against experimental results, shows consistency with values reported in the literature, particularly concerning the effectiveness of the reinforcement as a function of its configuration and application surface (intrados, extrados, or both).

Further experimental testing will carry out by applying the correction to the setup at the basement of the vault and also numerical analysis are needed to confirm the preliminary results obtained in this study.

## Acknowledgements

This paper was produced with the financial support under the National Recovery and Resilience Plan (NRRP), Mission 4, Component 2, Investment 1.1, funded by the European Union – NextGenerationEU– Project Title: sTructurAl and eneRGy rEnovation for susTainable buildingS - TARGETS – CUP B53D23027280001 Grant Assignment Decree No. 1409 adopted on 14.9.2022 by the Italian Ministry of University and Research (MUR)

## References

Alecci V, Misseri G, Rovero L, Stipo G, De Stefano M, Feo L, et al. 2016, Experimental investigation on masonry arches strengthened with PBO-FRCM composite. Compos B, 100:228–39

Boem, I., Gattesco, N. 2021. Cyclic behavior of masonry barrel vaults strengthened through Composite Reinforced Mortar, considering the role of the connection with the abutments. Engineering Structures 228:111518.

Boem, I., Gattesco, N., 2023, Composite Reinforced Mortar (CRM) and Fiber-Reinforced Cementitious Matrix (FRCM) for the seismic protection of masonry vaults, Procedia Structural Integrity 44, 1260–1267

Caceres-Vilca, G., Copa-Pineda, J., Copa-Pineda, F., Malaga-Chuquitaype, C. 2024. Experimental assessment of sillar masonry barrel vaults retrofitted with reinforced concrete elements. Structures 62:106145.

Cardinali V., Pintucchi, B., Tanganelli, M., Trovatelli, F. 2023, Settlement of masonry barrel vaults: an experimental and numerical study. Procedia Structural Integrity 44: 1252–1259.

Carozzi F. G., Poggi C., , Bertolesi E., Milani G., 2018, Ancient masonry arches and vaults strengthened with TRM, SRG and FRP composites: Experimental evaluation, Composite Structures, Volume 187, 466-480

Castellano, A., Fraddosio, A., Oliveira, D. V., Piccioni, M. D., Ricci, E., & Sacco, E. 2023, An effective numerical modelling strategy for FRCM strengthened curved masonry structures. Engineering Structures, 274, 115116.

De Santis S, de Roscini F, Felice G. 2017, Retrofitting masonry vaults with basalt textile reinforced mortar. Key Eng Mater, 747:250–7

Garmendia, L., Larrinaga, P., San-Mateos, R., San-Josè, J.T.,.2015, Strengthening masonry vaults with organic and inorganic composites: an experimental approach. Materials & Design, 85, 102–14

Gattesco, N., Boem, I., Andretta, V. 2018. Experimental behaviour of non-structural masonry vaults reinforced through fibre-reinforced mortar coating and subjected to cyclic horizontal loads. Eng Struct 172:419–31.

Heyman, J. 1966, The stone skeleton. International Journal of solids and structures, 2(2), 249-279.

La Mendola, L., Failla, A., Cucchiara, C., Accardi, M. 2009. Debonding phenomena in CFRP strengthened calcarenite masonry walls and vaults. Advances in Structural Engineering 12(5): 745–760.

Lourenço, P. B. 2010, Recent advances in masonry modelling: micromodelling and homogenisation. Multiscale modeling in solid mechanics: computational approaches, 251-294.

Lourenço, P. B., & Rots, J. 1994, Analysis of masonry structures with interface elements. Rep. No. 03-21-22-0, 1.

Marini, A., Belleri, A., Preti, M., Riva, P., Giuriani, E. 2017. Lightweight extrados restraining elements for the anti-seismic retrofit of single leaf vaults. Engineering Structures 141:543–554.

MIDAS Information Technology, Co., Ltd., 2022, MIDAS FEA NX Manual, CSP FEA, Este (PD), Italy.

Minafò, G., & La Mendola, L. 2018, Experimental investigation on the effect of mortar grade on the compressive behaviour of FRCM confined masonry columns. Composites Part B: Engineering, 146, 1-12.

UNI EN 12664:2002. Thermal performance of building materials and products. Determination of thermal resistance by means of guarded hot plate and heat flow meter methods - Dry and moist products of medium and low thermal resistance.

UNI EN 12667:2002. Thermal performance of building materials and products: Determination of thermal resistance by means of guarded hot plate and heat flow meter methods - Products of high and medium thermal resistance.

UNI (2006) EN 1926. Natural stone test methods – determination of uniaxial compressive strength

UNI (2006) EN 1015-11:1999/A1. Methods of test for mortar for masonry - Part 11: Determination of flexural and compressive strength of hardened mortar.

Ramaglia, G., Lignola, G.P., Prota, A. 2016. Collapse analysis of slender masonry barrel vaults. Engineering Structures 117: 86–100

Standard Test Method for Compressive Strength for Laboratory Constructed Masonry Prisms, ASTM E 447- 97. 1997, American Society for Testing and Materials

Zampieri, P., Simoncello, N., Tetougueni, C. D., Pellegrino, C. 2018, A review of methods for strengthening of masonry arches with composite materials, Engineering Structures 171, 154–169